High repetition granular Co/Pt multilayers with improved perpendicular remanent magnetization for high-density magnetic recording

Zhi Li(李智)[1,2], Kun Zhang(张昆)[1,2,†], Ao Du(杜奥)[1], Hongchao Zhang(张洪超)[1,2], Weibin Chen(陈伟斌)[3], Ning Xu(徐宁)[1,2], Runrun Hao(郝润润)[2], Shishen Yan(颜世申)[3], Weisheng Zhao(赵巍胜)[1,2], and Qunwen Leng(冷群文)[1,2]

[1] *Fert Beijing Research Institute, MIIT Key Laboratory of Spintronics, School of Integrated Circuit Science and Engineering, Beihang University, Beijing* 100191, *China*

[2] *Beihang–Goertek Joint Microelectronics Institute, Qingdao Research Institute, Beihang University, Qingdao* 266101, *China*

[3] *School of Physics, State Key Laboratory of Crystal Materials, Shandong University, Jinan* 250100, *China*

(Received 7 September 2022; revised manuscript received 24 October 2022; accepted manuscript online 3 November 2022)

Thanks to the strong perpendicular magnetic anisotropy (PMA), excellent processing compatibility as well as novel spintronic phenomenon, Co/Pt multilayers have been attracting massive attention and widely used in magnetic storage. However, reversed magnetic domains come into being with the increasing layer repetition 'N' to reduce magneto-static energy, resulting in the remarkable diminishment of the remanent magnetization (M_r). As a result, the product of M_r and thickness (*i.e.*, the remanent moment-thickness product, M_rt), a key parameter in magnetic recording for reliable data storing and reading, also decreases dramatically. To overcome this issue, we deposit an ultra-thick granular $[Co/Pt]_{80}$ multilayer with a total thickness of 68 nm on granular SiN_x buffer layer. The M_rt value, M_r to saturation magnetization (M_s) ratio as well as out of plane (OOP) coercivity (H_{coop}) are high up to 2.97 memu/cm^2, 67%, and 1940 Oe (1 Oe = 79.5775 A·m^{-1}), respectively, which is remarkably improved compared with that of continuous $[Co/Pt]_{80}$ multilayers. That is because large amounts of grain boundaries in the granular multilayers can efficiently impede the propagation and expansion of reversed magnetic domains, which is verified by experimental investigations and micromagnetic simulation results. The simulation results also indicate that the value of M_rt, M_r/M_s ratio, and H_{coop} can be further improved through optimizing the granule size, which can be experimentally realized by manipulating the process parameter of SiN_x buffer layer. This work provides an alternative solution for achieving high M_rt value in ultra-thick Co/Pt multilayers, which is of unneglectable potential in applications of high-density magnetic recording.

Keywords: granular Co/Pt multilayers, perpendicular magnetic anisotropy, remanent moment-thickness product, magnetic recording

PACS: 68.65.Ac, 68.65.Cd, 75.50.Ss, 75.60.Jk **DOI:** 10.1088/1674-1056/ac9fc1

1. Introduction

Co/Pt multilayers have been attracting large amounts of attentions because of its great interest in fundamental physics, such as spin–orbit torque effect, magnetic skyrmions and synthetic antiferromagnetic structure, as well as its great application potential in magnetic recording and magnetic random-access memories (MRAM).[1–11] The strong perpendicular magnetic anisotropy (PMA) and excellent processing compatibility of Co/Pt multilayers are urgently desired by the application of high-density magnetic recording medium. However, the out of plane (OOP) magnetic hysteresis (M–H) loop of Co/Pt multilayers transforms from a rectangular shape to a bowknot shape with the increasing repetition number, leading to the remarkable reduction of remanent magnetization (M_r). Note that, the product of M_r and thickness (*i.e.*, the remanent moment-thickness product, M_rt) is a key parameter in magnetic recording for high signal-to-noise data reading and high-density information storage, which also decreases dramatically with the increasing repetition number.[12] This is because that the magneto-static energy increases linearly with the increasing repetition number of Co/Pt multilayers, reversed magnetic domains come into being, and the M_rt value is normally restricted to lower than 0.5 memu/cm^2. Therefore, there is always a contradiction point between the M_rt value and the repetition number of Co/Pt multilayers, which hinders its further practical applications in high-density magnetic recording.[13–16]

Recently, many researches focus on improving the magnetic performance of Co/Pt multilayers for magnetic recording. For example, patterned microstructures and nanoporous substrates are utilized for fabricating Co/Pt multilayers, whose coercivity is enhanced by optimizing the size of dot or nanopore.[17,18] Meanwhile, interface-degradation-induced irreversible PMA loss of Co/Pt multilayers during high-temperature annealing are investigated.[19] Moreover, the optimization of PMA in Co/Pt multilayers is studied to improve their thermal stability. For instance, Co/Pt multilayers with strong PMA can be achieved by the strategy of exchange bi-

[†]Corresponding author. E-mail: zhang_kun@buaa.edu.cn

© 2023 Chinese Physical Society and IOP Publishing Ltd

ased structure, or by optimizing interface quality.[20,21] However, the magnetic performance of Co/Pt multilayers with high total thickness is seldom studied.

In this work, high repetition $[Co/Pt]_{80}$ multilayers with total thickness of 68 nm are deposited on granular SiN_x buffer layer by magnetron sputtering technology. As a result, the magnetic parameters, such as $M_r t$, OOP coercivity (H_{coop}), and M_r to saturation magnetization (M_s) ratio, are significantly improved compared with that of a continuous multilayer on smooth substrate. The magnetic domain characterization and micromagnetic simulation indicate that granular microstructure brings large amounts of grain boundaries, which can efficiently impede the expansion and propagation of reversed magnetic domains to improve the magnetic performance. Moreover, the magnetic performance of granular $[Co/Pt]_{80}$ multilayers can be further improved through tuning the granular microstructure of SiN_x buffer layer, which can be realized by controlling the deposition parameters. This work implements excellent magnetic performance in high repetition Co/Pt multilayers, which can promote the development of high-density magnetic recording mediums.

2. Methods

2.1. Film preparation

The 100-nm SiN_x buffer layer is deposited on silicon wafer at 350 °C by ULVAC CC-200Cz PECVD system. The flow ratio of SiH_4 and NH_3 is set as 4:5, and the deposition pressure of the SiN_x layer is 1 Torr (1 Torr = 1.33322×10^2 Pa), which introduces a granular surface structure.[22] Ta(2.0 nm)/Pt(1.5 nm)/$[Co(0.5\ nm)/Pt(0.35\ nm)]_N$ multilayers are then deposited on granular Si/SiN_x substrates at room temperature by Singulus ROTARIS sputtering system with a base pressure of 5×10^{-8} Torr. Comparison samples with coordinating film structure are deposited on smooth Si/SiO_2 substrates. The deposition rate is 0.87 Å/s for Co and 1.21 Å/s for Pt, respectively.

2.2. Structural and magnetic characterizations

The magnetic hysteresis (M–H) loops are measured by a vibration sample magnetometer (VSM) from Lake Shore company. The Bruker Dimension Icon atomic force microscope (AFM) and Zeiss Sigma 300 scanning electron microscope (SEM) are used to analyze the surface morphology. The magnetic force microscope (MFM) measurement for magnetic structure characterization is accomplished by Bruker Dimension Icon. All the characterizations are operated at room temperature.

3. Results and discussion

3.1. Improved magnetic properties in granular $[Co/Pt]_N$ multilayers

Figures 1(a) and 1(b) exhibits the OOP M–H loops of $[Co/Pt]_N$ multilayers. Obviously, the OOP M–H loops of granular and continuous $[Co/Pt]_N$ multilayers respectively exhibit rectangular and bowknot shape. As a result, the values of H_{coop} and M_r/M_s ratio for granular $[Co/Pt]_N$ multilayers are remarkably improved compared with that of continuous $[Co/Pt]_N$ multilayers. For example, the value of H_{coop} and M_r/M_s ratio are improved from 204 Oe and 17.0% to 1780 Oe and 69.4% for $N = 60$. Similarly, the value of H_{coop} and M_r/M_s ratio are improved from 216 Oe and 14.6% to 1940 Oe and 67.0% for $N = 80$.

Figures 1(c) and 1(d) show the MFM images of granular and continuous $[Co/Pt]_{80}$ multilayers, respectively. The specimens are OOP saturated by electromagnet and investigated at remanent magnetization state. The bright and dark pixels represent the positive and negative magnetized regions. The corresponding AFM results, *i.e.*, the surface structure of the measured area, can be found in inserts. The MFM results are independent of the surface morphology, so the disturbance of the surface structure in the MFM results can be excluded. Maze domains can be clearly observed in the continuous $[Co/Pt]_{80}$ multilayers, and a weak remanent magnetization state is determined by the unconstrained domain nucleation and propagation. For the granular $[Co/Pt]_{80}$ multilayers, the nonuniform deposition at the grain boundaries induces soft magnet phase, resulting in a reduced exchange stiffness A_{ex}, saturation magnetization M_s, and perpendicular magnetic anisotropy constant K_u.[17,23,24] Meanwhile, the critical domain wall propagation field is in negative relationship with the above-mentioned parameters.[25] Therefore, the critical domain wall propagation field is enlarged. That means the propagation and expansion of reversed magnetic domains are impeded by the grain boundaries and a higher M_r/M_s ratio is achieved. Moreover, because of the pinning effect of grain boundaries, a higher external magnetic field will be essential to expand the reversed magnetic domains, and a stronger H_{coop} can be expected.

Furthermore, the tendency of M_r/M_s ratio, H_{coop} and $M_r t$ varying with the repetition number N from 10 to 80 are systematically investigated, as shown in Figs. 2(a)–2(c). For continuous Co/Pt multilayers, the H_{coop} experiences a linear augment with increasing N, which is attributed to the slower domain propagation under a higher total film thickness.[13] The M_r/M_s ratio can reach about 100% when $N = 10$ and 30, and a maximum $M_r t$ is observed as 1.695 memu/cm^2 for $N = 30$. However, a sharp decline occurs when N exceeds 30, which can be clearly observed in the OOP M–H loops shown in Fig. 2(d). This phenomenon can be attributed to the increased magneto-static energy ($E_{mag-sta}$) with uniform

magnetization[26]

$$E_{\mathrm{mag-sta}} = -\frac{\boldsymbol{H}_{\mathrm{demag}} \cdot \boldsymbol{M}}{2} = 2\pi M_{\mathrm{S}}^2 t, \tag{1}$$

where $\boldsymbol{H}_{\mathrm{demag}}$, $\boldsymbol{M}$, and t refer to the demagnetization field, magnetization, and layer thickness, respectively. With the increasing thickness, the magneto-static energy $E_{\mathrm{mag-sta}}$ increases dramatically if the multilayers sustain a saturation magnetization state. As a result, the strong demagnetization field $\boldsymbol{H}_{\mathrm{demag}}$ force the premature nucleation of reversed magnetic domain, *i.e.*, the irreversible magnetization switching, resulting in the reduced M_{r}. For the granular multilayers, the $M_{\mathrm{r}}/M_{\mathrm{s}}$ ratio and $M_{\mathrm{r}}t$ for $N = 10$ and 30 are similar to those of continuous multilayers, while their H_{coop} slightly increase due to the granule structure. Excitingly, for $N = 60$ and 80, it can be extracted that $M_{\mathrm{r}}/M_{\mathrm{s}}$ ratio, H_{coop}, and $M_{\mathrm{r}}t$ are remarkably enhanced. It is worth noting that $M_{\mathrm{r}}t$ value in this work is observed as high as 2.97 memu/cm^2 for granular multilayer with $N = 80$, which is a new record in Co/Pt multilayer systems to our knowledge.

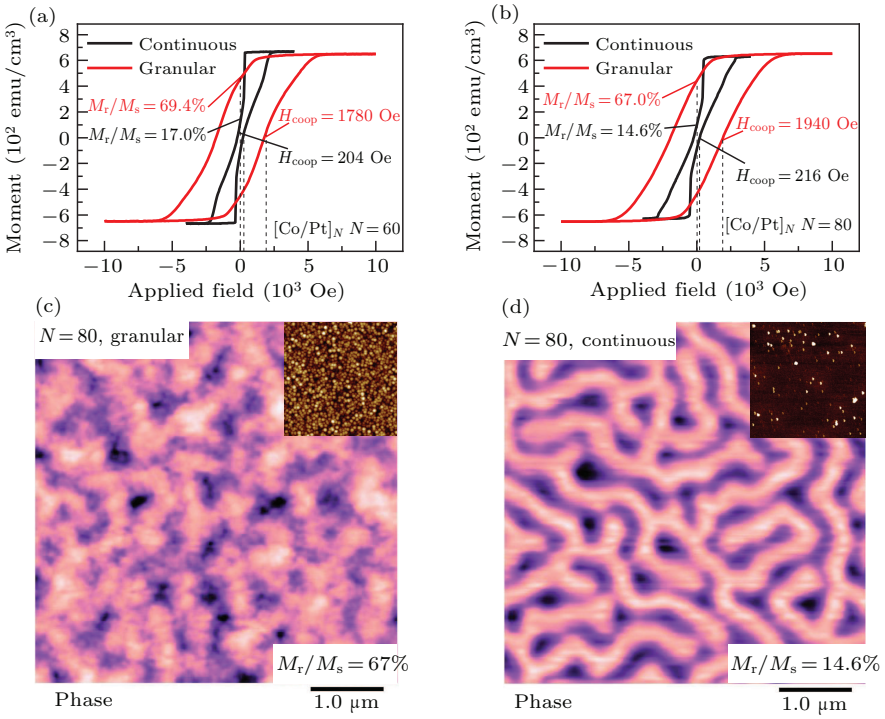


Fig. 1. (a) and (b) OOP M–H loops of the granular and continuous $[Co/Pt]_N$ multilayers with $N = 60$ and 80. The data of the granular and continuous multilayers are marked as red and black, respectively. (c) and (d) MFM image of granular and continuous $[Co/Pt]_{80}$ multilayers under zero external field after a saturate magnetization, *i.e.*, the remanent magnetization state. The corresponding AFM graphs are inserted at the upper-right corner of the images.

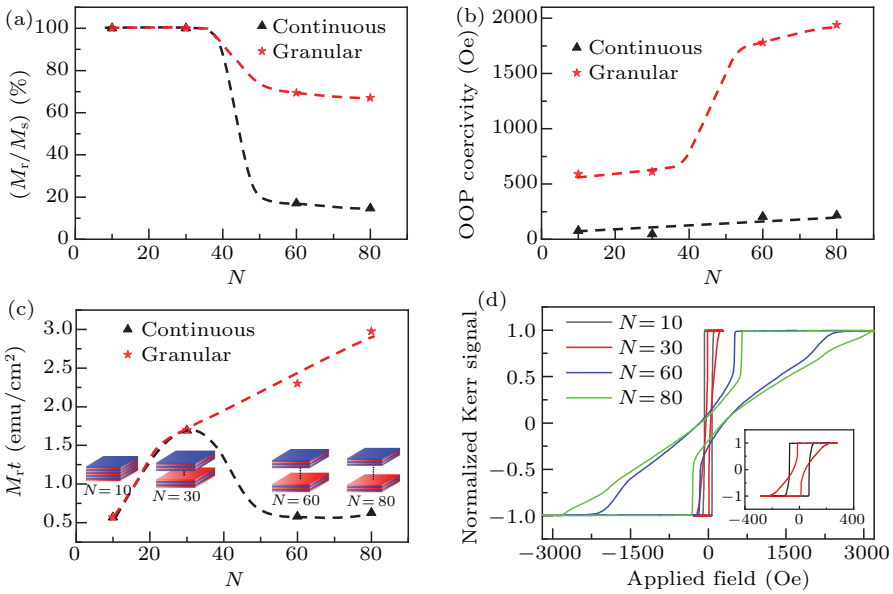


Fig. 2. The relationship of repetition number N *versus* (a) $M_{\mathrm{r}}/M_{\mathrm{s}}$, (b) H_{coop}, and (c) $M_{\mathrm{r}}t$ of the granular and continuous Co/Pt multilayers. (d) OOP M–H loops of continuous Co/Pt multilayers with different repetition numbers. The inserted picture exhibits the zoomed graph of continuous Co/Pt multilayers with $N = 10$ and 30.

3.2. Surface morphology of granular SiN_x layer and $[Co/Pt]_N$ multilayers

To well understand the origin of granular structure, we investigate the surface morphology of granular SiN_x buffer layer and $[Co/Pt]_N$ multilayers. As exhibited in Fig. 3(a), granular morphology is formed on the SiN_x layer by PECVD process. The $[Co/Pt]_{80}$ multilayers are then deposited on the granules. In this case, the granular morphology is transferred from the SiN_x buffer layer to the $[Co/Pt]_N$ multilayers as shown in Fig. 3(b). The surface roughness (*i.e.*, R_a) of granular SiN_x layer and Co/Pt multilayers are 5.59 nm and 5.88 nm, respectively. As a contrast, the surface roughness of smooth SiO_2 buffer layer and continuous $[Co/Pt]_{80}$ multilayers are only about 0.11 nm and 0.50 nm, as shown in Fig. 3(c). Here, the consistent roughness of SiN_x buffer layer and granular $[Co/Pt]_{80}$ multilayers indicate the layer-by-layer deposition mode and high depositing quality of the magnetic layers. Therefore, PMA in our granular Co/Pt multilayers can be attributed to the Co/Pt interfacial orbital hybridization.[27] Meanwhile, the bulk PMA originating from magnetocrystalline anisotropy can be excluded in this work because that the multilayers do not go through any hightemperature treatment, which is essential for the formation of PMA CoPt alloys with specific crystalline structure.[28,29]

The granule size distributions of granular substrate and $[Co/Pt]_{80}$ multilayers are illustrated in Figs. 3(d) and 3(e), that is measured as average dimension $d = 105.7$ nm and 103.9 nm with a standard deviation of 14.7% and 22.2%, respectively. The granule size here is defined by the average of Feret's diameter, and is retained after the deposition of the Co/Pt multilayer while a remarkable increase of the standard deviation is confirmed. The reason of this phenomenon can be attributed to the flattening effect of Co/Pt multilayers. During the deposition process, the magnetic film is formed on both the surface and the gap of granules. The irregular film formation on the granular surface changes the uniformity of the magnetic layers, and meanwhile builds a barrier for impeding the domain propagation and expansion during the reversal of magnetic moment. Moreover, the surface structure of granular $[Co/Pt]_{80}$ multilayer is also studied by SEM with 45° incident electron beam to the film normal. The granular $[Co/Pt]_{80}$ multilayer with SiN_x buffer layer are clearly observed on the smooth Si substrate. The height of the granules can be estimated as 160 nm, which is accordance with the total thickness of SiN_x and $[Co/Pt]_{80}$ layers. Something should be noted that, the surface structure of the SiN_x buffer layer including surface roughness, granule size, and distribution can be further manipulated by adjusting the process parameters. As can be easily understood, high deposition rate of the SiN_x film leads to a limited film condition and high granule size, which can be achieved by high RF power, depositing chamber pressure, and SiH_4 proportion. On the contrary, lower granule size can be achieved by decreasing the aforesaid parameters.[30,31] Therefore, the magnetic performance of granular $[Co/Pt]_N$ multilayers can be further optimized technically.

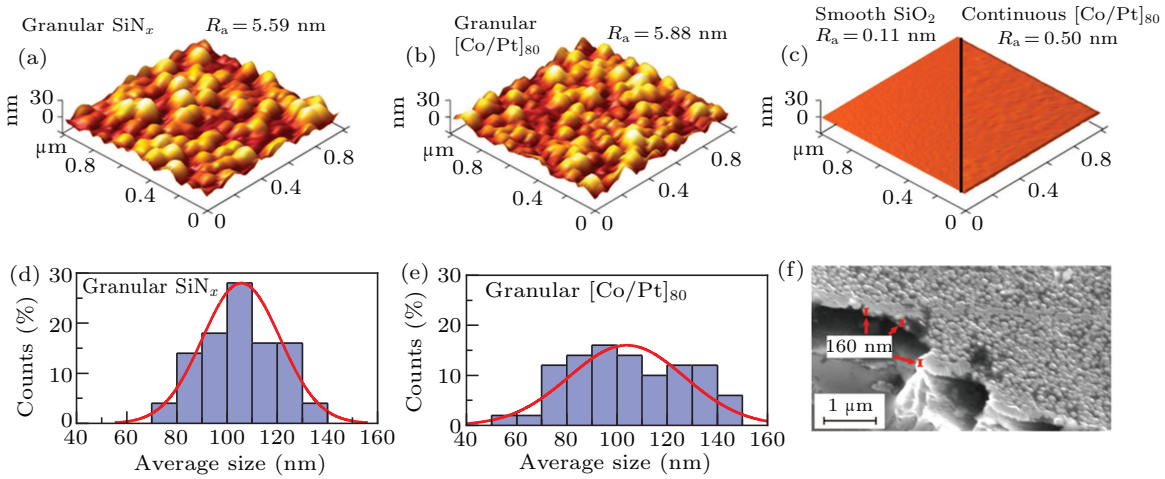


Fig. 3. (a) and (b) Surface structure of granular SiN_x buffer layer and granular $[Co/Pt]_{80}$ multilayer. (c) AFM image of smooth SiO_2 buffer layer and continuous $[Co/Pt]_{80}$ multilayer, respectively. (d) and (e) The granule size distribution of granular SiN_x buffer layer and granular $[Co/Pt]_{80}$ multilayer. (f) The SEM image of granular $[Co/Pt]_{80}$ multilayer measured with 45° incident electron beam to the film normal.

3.3. Micromagnetic simulation and theoretical analyses

To further clarify the relationship between the granule size and the magnetic properties of granular $[Co/Pt]_N$ multilayers, a micromagnetic model is established and simulated by Object Oriented MicroMagnetic Framework (OOMMF).[32] The simulation region is set as 500 nm×500 nm×68 nm with a cell size of 2 nm, and the parameters of exchange coefficient A_{ex}, saturation magnetization M_s, damping coefficient α, and simulation temperature T are set to be 1×10^{-11} J/m, 6.5×10^5 A/m, 1, and 300 K, respectively. The granular structure is imitated by gridded hexagonal units with their boundary of a lower M_s, *i.e.*, one-tenth of the normal value. It should be mentioned that the granule size here is defined as the average of the long axis and short axis of hexagonal units. The ex-

change coupling at the boundary is thus restricted and the domain propagation and expansion is hindered by this granular boundary.

The simulated M–H loops of continuous and granular $[Co/Pt]_N$ multilayers are exhibited in Fig. 4(a), which are consistent with the experimental observations. The continuous film experience lowest M_r/M_s and H_{coop}, that are typical in Co/Pt multilayers with high repetition N.[14,33] The aforesaid parameters are enhanced from 6.7% and 413 Oe to 60% and 667 Oe, respectively in simulated granular films with granular size of 80 nm. In this case, the value of M_rt is improved simultaneously with M_r/M_s ratio because that the value of t and M_s stays constant. For further investigation of the relationship between granule size and magnetic performances, magnetic reversals with different granular sizes, *i.e.*, the hexagon size, are studied. A rectangular M–H loops with 100% M_r/M_s ratio and 5500-Oe H_{coop} is achieved for the granular $[Co/Pt]_N$ multilayers with granule size 20 nm. As illustrated in Figs. 4(b) and 4(c), the value of H_{coop} and M_r/M_s decline with the increase of the granule size. These simulation results indicate that the magnetic property of granular $[Co/Pt]_N$ multilayers can be further improved through reducing the granule size.

To study the dynamic process of the magnetic reversal in granular $[Co/Pt]_N$ multilayers, the reversed domain nucleation and propagation processes are schematically studied, as shown in Figs. 4(d)–4(i). For the state of points 1 and a in Fig. 4(a), the reversed magnetic domains nucleate and expand, and a multi-domain state is established under zero external field, *i.e.*, the remanent magnetization state. The reversed domain propagation is restrained by the grain boundary in granular film and an improved remanent magnetization is observed. Subsequently, a negative OOP field is applied at points 2 and b, and the total magnetization along z axis becomes zero, *i.e.*, the coercivity field state. A stronger external field is essential to achieve a zero perpendicular magnetization due to the inhibition of reversed domain propagation and expansion, and the coercivity is enhanced. For a stronger negative OOP field at points 3 and c, the positive domain starts to shrink and annihilate, and the magnetization state approaches reversed saturation state. A smoother shrinking process can be observed in the granular multilayer, which is due to the reduced exchange coupling at the grain boundaries.

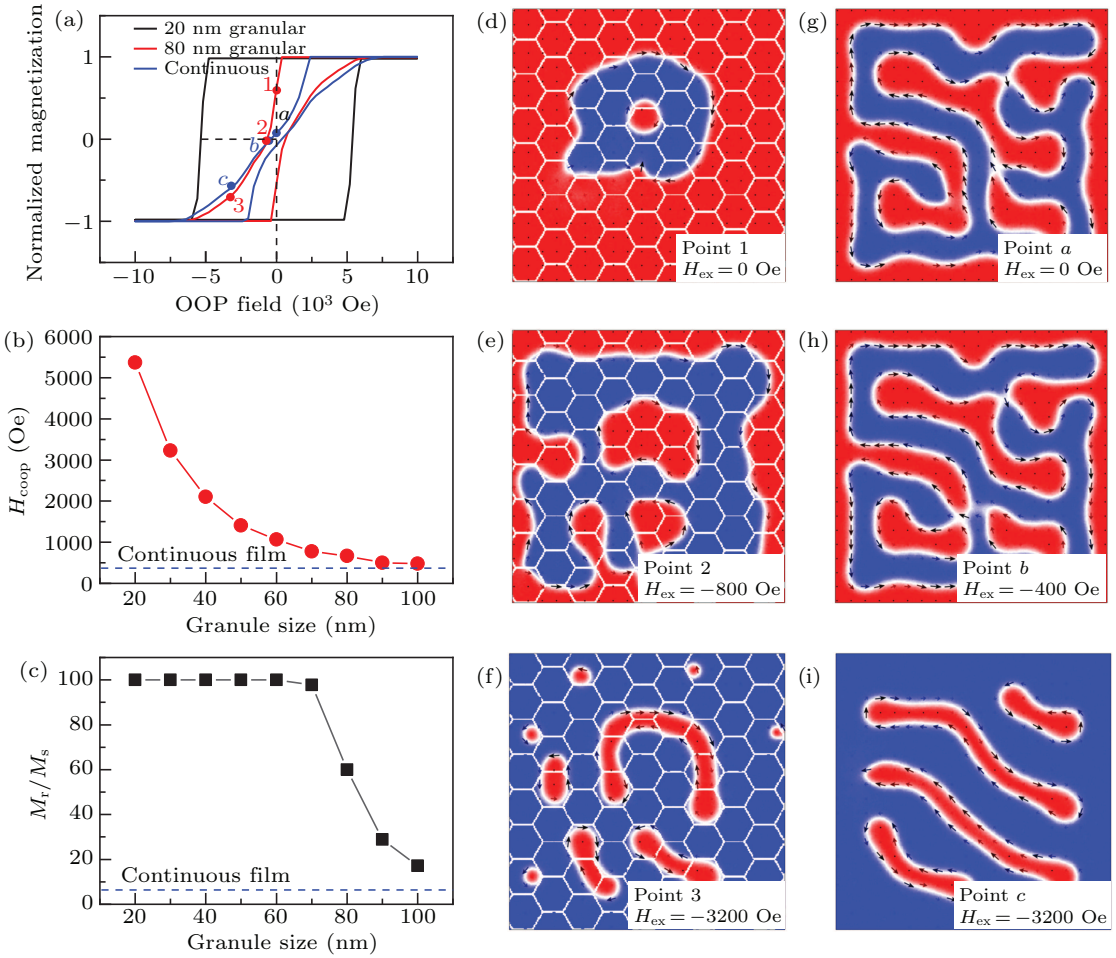


Fig. 4. (a) The simulated OOP M–H loops of Co/Pt multilayers with different surface structures. (b) and (c) The tendency of H_{coop} and M_r/M_s with increasing granule size. The blue dotted line represents the data extracted from continuous Co/Pt multilayers. (d)–(f) The magnetic domain reversal dynamics in Co/Pt multilayers with a granule size of 80 nm. (g)–(i) The magnetic domain reversal dynamics in continuous Co/Pt multilayers. The corresponding states are illustrated in panel (a) as points 1–3 for granular film and points a–c for continuous film. The red and blue areas refer to the spin-up and spin-down states, respectively.

4. Conclusion and perspectives

High repetition $[Co/Pt]_N$ multilayers with PMA are experimentally fabricated, in which the key magnetic performance such as $M_r t$, M_r/M_s ratio, and H_{coop} are remarkably improved benefiting from the granular structure. The corresponding simulation results indicate that the magnetic parameters can be optimized by modifying the granule size. This research gives a new method to optimize the magnetic performance of Co/Pt multilayers with high total thickness, which exhibits strong potential in the application of high-density magnetic recording.

Acknowledgements

Project supported by the National Natural Science Foundation of China (Grant No. 51901008) and the National Key Research and Development Program of China (Grant No. 2021YFB3201800).

References

[1] Wang X, Cao A, Li S, Tang J, Du A, Cheng H, Sun Y, Du H, Zhang X and Zhao W 2021 *Phys. Rev. B* **104** 064421
[2] Wang M X, Cai W L, Cao K H, Zhou J Q, Wrona J, Peng S Z, Yang H W, Wei J Q, Kang W, Zhang Y G, Langer J, Ocker B, Fert A and Zhao W S 2018 *Nat. Commun.* **9** 1
[3] Wang M X, Cai W L, Zhu D Q, Wang Z H, Kan J, Zhao Z Y, Cao K H, Wang Z L, Zhang Y G, Zhang T R, Park C, Wang J P, Fert A and Zhao W S 2018 *Nat. Electron.* **1** 582
[4] Zhang X, Cai W, Zhang X, Wang Z, Li Z, Zhang Y, Cao K, Lei N, Kang W, Zhang Y, Yu H, Zhou Y and Zhao W 2018 *ACS Appl. Mater. Interfaces* **10** 16887
[5] Fallarino L, Oelschlägel A, Arregi J A, Bashkatov A, Samad F, Böhm B, Chesnel K and Hellwig O 2019 *Phys. Rev. B* **99** 024431
[6] Xie X, Zhao X, Dong Y, Qu X, Zheng K, Han X, Han X, Fan Y, Bai L, Chen Y, Dai Y, Tian Y and Yan S 2021 *Nat. Commun.* **12** 2473
[7] Iihama S, Xu Y, Deb M, Malinowski G, Hehn M, Gorchon J, Fullerton E E and Mangin S 2018 *Adv. Mater.* **30** 1804004
[8] Zhang K, Chen L, Zhang Y, Hong B, He Y, Lin K, Zhang Z, Zheng Z, Feng X and Zhang Y 2022 *Appl. Phys. Rev.* **9** 011407
[9] Sato H, Ikeda S, Fukami S, Honjo H, Ishikawa S, Yamanouchi M, Mizunuma K, Matsukura F and Ohno H 2014 *Jpn. J. Appl. Phys.* **53** 4S
[10] Guo Z, Yin J, Bai Y, Zhu D, Shi K, Wang G, Cao K and Zhao W 2021 *Proc. IEEE* **PP(99)** 1398–1417
[11] Jiang Y, Zhou H, Zhu D, Wang C, Wang Z and Zhao W 2021 *IEEE International Electron Devices Meeting (IEDM)*, December 13–15, 2021, San Francisco, USA, p. 8.2.1
[12] Hono K, Takahashi Y K, Ju G, Thiele J U, Ajan A, Yang X, Ruiz R and Wan L 2018 *MRS Bull.* **43** 93
[13] Knepper J W and Yang F Y 2005 *Phys. Rev. B* **71** 224403
[14] Davies J E, Hellwig O, Fullerton E E, Denbeaux G, Kortright J B and Liu K 2004 *Phys. Rev. B* **70** 224434
[15] Stillrich H, Menk C, Frömter R and Oepen H P 2009 *J. Appl. Phys.* **105** 07C308
[16] Alex M, Tselikov A, Mcdaniel T, Deeman N, Valet T and Chen D 2001 *IEEE Trans. Magn.* **37** 1244
[17] Nguyen T N A, Fedotova J, Kasiuk J, Bayev V, Kupreeva O, Lazarouk S, Manh D H, Vu D L, Chung S, Åkerman J, Altynov V and Maximenko A 2018 *Appl. Surf. Sci.* **427** 649
[18] Zhu F Q, Shang Z, Monet D and Chien C L 2007 *J. Appl. Phys.* **101** 09J101
[19] Figueiredo-Prestes N, Zarpellon J, Costa D d S, Mazzaro I, de Camargo P C, de Oliveira A J A, Deranlot C, George J M and Mosca D H 2021 *J. Phys. Chem. C* **125** 4885
[20] Yıldırım O, Marioni M A, Falub C V, Rohrmann H, Jaeger D, Rechsteiner M, Schneider D and Hug H J 2022 *Scr. Mater.* **207** 114285
[21] Feng J, Liu H F, Wei H X, Zhang X G, Ren Y, Li X, Wang Y, Wang J P and Han X F 2017 *Phys. Rev. Appl.* **7** 054005
[22] Wuu D S, Lo W C, Chiang C C, Lin H B, Chang L S, Horng R H, Huang C L and Gao Y J 2005 *Surf. Coat. Technol.* **198** 114
[23] Zhang J, Sun Z, Sun J, Kang S, Yu S, Han G, Yan S, Mei L and Li D 2013 *Appl. Phys. Lett.* **102** 152407
[24] Rahman M T, Dumas R K, Eibagi N, Shams N N, Wu Y C, Liu K and Lai C H 2009 *Appl. Phys. Lett.* **94** 042507
[25] Mohakud S, Andraus S, Nishino M, Sakuma A and Miyashita S 2016 *Phys. Rev. B* **94** 054430
[26] Hellwig O, Berger A, Kortright J B and Fullerton E E 2007 *J. Magn. Magn. Mater.* **319** 13
[27] Zarpellon J, Jaffrès H, Frougier J, Deranlot C, George J M, Mosca D H, Lemaître A, Freimuth F, Duong Q H, Renucci P and Marie X 2012 *Phys. Rev. B* **86** 205314
[28] Belle B D, Schedin F, Pilet N, Ashworth T V, Hill E W, Nutter P W, Hug H J and Miles J J 2007 *J. Appl. Phys.* **101** 09F517
[29] Thomson T, Hu G and Terris B D 2006 *Phys. Rev. Lett.* **96** 257204
[30] Besland M P, Lapeyrade M, Delmotte F and Hollinger G 2004 *J. Vac. Sci. Technol. A* **22** 1962
[31] Carcia P F, McLean R S, Groner M D, Dameron A A and George S M 2009 *J. Appl. Phys.* **106** 023533
[32] Donahue M J and Porter D G 1999 *OOMMF user's guide*, Version 1.0
[33] Fromter R, Stillrich H, Menk C and Oepen H P 2008 *Phys. Rev. Lett.* **100** 207202